POLITECNICO DI TORINO
Repository ISTITUZIONALE

Study of wheel-rail adhesion during braking maneuvers

Original
Study of wheel-rail adhesion during braking maneuvers / Bosso, N., Gugliotta, A., Magelli, M., Oresta, I.F., Zampieri, N.. - In: PROCEDIA STRUCTURAL INTEGRITY. - ISSN 2452-3216. - ELETTRONICO. - 24:(2019), pp. 680-691. (48th International Conference on Stress Analysis, AIAS 2019 Assisi 2019) [10.1016/j.prostr.2020.02.060].

Availability:
This version is available at: 11583/2859058 since: 2020-12-27T15:45:15Z

Publisher:
Elsevier B.V.

Published
DOI:10.1016/j.prostr.2020.02.060

Terms of use:

This article is made available under terms and conditions as specified in the corresponding bibliographic description in the repository

Publisher copyright

(Article begins on next page)

09 November 2026

Available online at www.sciencedirect.com

ScienceDirect

Procedia Structural Integrity 24 (2019) 680–691

Structural Integrity Procedia

www.elsevier.com/locate/procedia

AIAS 2019 International Conference on Stress Analysis

Study of wheel-rail adhesion during braking maneuvers

Nicola Bosso[a], Antonio Gugliotta[a], Matteo Magelli[a], Italo Francesco Oresta[a], Nicolò Zampieri[a]*

[a]*Department of Mechanical and Aerospace Engineering, Politecnico di Torino, C.so Duca degli Abruzzi 24, Torino 10129, Italy*

Abstract

The present work aims to better understand the phenomenon of adhesion under degraded conditions during railway braking maneuvers with the aim of optimizing the anti-slip algorithms in order to reduce damage to the profiles of wheels and rails and to minimize the braking distance. The proposed approach is based on the analysis of experimental data acquired during braking tests carried out on track, considering different types of vehicles and different types of contaminants, able to reproduce the typical degraded adhesion conditions occurring during normal operation. The work describes a numerical model that allows to evaluate the dynamics of the vehicle during the braking operation and to correlate the pressures to the brake cylinder, which are related to the braking forces, and the angular velocities measured on the axles of the vehicle, with the adhesion coefficient.

© 2019 The Authors. Published by Elsevier B.V.
This is an open access article under the CC BY-NC-ND license (http://creativecommons.org/licenses/by-nc-nd/4.0/)
Peer-review under responsibility of the AIAS2019 organizers

Keywords: Wheel-rail adhesion; WSP systems; degraded adhesion; adhesion recovery; railway braking

1. Introduction

The forces generated at the wheel-rail interface represent one of the most interesting aspects within railway research, as they influence the dynamic behaviour of the vehicle, playing a fundamental role during the traction and braking maneuvers. The calculation of these forces is an extremely complex task due to the variability of the contact conditions and the presence of different types of contaminants. The contact between wheel and rail takes place in an open environment: this means that at the interface there may be elements coming from outside, which inevitably

* Corresponding author. Tel.: +39-011-090-6997; fax: +39-011-090-6999.
E-mail address: nicolo.zampieri@polito.it

2452-3216 © 2019 The Authors. Published by Elsevier B.V.
This is an open access article under the CC BY-NC-ND license (http://creativecommons.org/licenses/by-nc-nd/4.0/)
Peer-review under responsibility of the AIAS2019 organizers
10.1016/j.prostr.2020.02.060

modify the adhesion conditions, generating an intermediate layer of material between the two surfaces in contact (Third body material, TBM). It is important to emphasize that often these TBMs interact chemically with the wheel and rail steels and consequently, the materials in contact have different chemical, mechanical and physical properties compared to the nominal ones in the absence of the contaminant, as described by Olofsson et al. (2013). The ratio between longitudinal and normal forces, called adhesion coefficient, therefore strongly depends on any substances lying at the wheel-rail interface, such as water, oil, grease, leaves and snow. This last aspect significantly affects the safety of the vehicle and for this reason there are many studies in the literature related to the variation of the adhesion coefficient under degraded conditions. In fact, the manufacturers of braking systems need to ensure that the vehicle is always able, under any conditions, to brake efficiently within the limits set by the standards UNI (2011) and UIC (2016). Low adherence occurs when the available friction is insufficient in order to satisfy a specific braking request. The available adhesion is therefore limited by the friction coefficient, which strongly depends on the contact conditions and therefore on the type of contaminant present on the rail. For this reason, sand and engineered products, called friction modifiers, are scattered at the wheel-rail interface respectively to increase adhesion and to maintain it at a constant optimum value. Furthermore, modern vehicles have mechatronic systems that have the task of maximizing performance and safety, in both traction (Antiskid) and braking (Wheel Slide Protection, WSP) maneuvers. The operation of these devices is based on a correct distribution of traction braking effort between the different wheels of the whole train. The experimental study of degraded adhesion is therefore an aspect of great importance in order to correctly predict the behaviour of a vehicle that runs on a contaminated section of track. However, this is not a simple task due to the complexity of the phenomenon, which becomes even more difficult if we consider the phenomenon of adhesion recovery. In fact, the first wheels of the vehicle have a cleaning effect on the surface of the rail that can determine a recovery of adhesion on the following wheelsets, as described by Bosso et al. (2015, 2016, 2019).

The authors Lewis and Olofsson (2009) provide an interesting classification of materials typically present at contact, distinguishing between contaminants, friction modifiers (FM) and lubricants. Contaminants are all those elements that are present at the interface due to climatic and environmental conditions, such as water, leaves, snow, but also debris due to surface wear, oxides, ballast gravel, dust, etc. All products, solid or liquid, which are intentionally spread on the wheel thread in order to achieve very precise friction values, are classified as FM.

Table 1. Values of friction coefficient obtained with tribometer Olofsson (2009).

Condition	Temperature (°C)	Friction coefficient
Dry rail	19	0.6-0.7
Wet rail	5	0.2-0.3
Grease	8	0.05-0.1
Leaves thin film	8	0.05-0.1

Table 2. Wheel-rail friction coefficient according to Moore (1975).

Rail condition	Friction coefficient
Clean dry rail	0.25-0.3
Rail and sand	0.25-0.33
Clean wet rail	0.18-0.20
Wet rail and sand	0.22-0.25
Grease	0.15-0.18
Dew	0.09-0.15
Snow	0.10
Snow and sand	0.15
Wet leaves	0.07

Finally, lubricants are defined as substances such as oil and grease that are intentionally spread on the flange of the wheel to reduce friction during cornering, in order to reduce wear and reduce the risk of derailment. In any case, Harmon and Lewis (2016) underline how we can distinguish between naturally present elements and products intentionally spread between wheel and rail to improve the vehicle performances in terms of grip, wear, safety, etc. There are numerous studies and articles in the literature that analyse adhesion conditions in the presence of contaminants; in particular, the results obtained by Olofsson (2009) are reported in Tab. 1 and 2 with a tribometer and by Moore (1975).

Also, in the Fulford (2004) publication for Railway Safety and Standard Boards (RSSB), some values of friction coefficient are reported considering different contamination conditions. The authors report a friction coefficient in the range 0.4-0.65 in dry condition and lower than 0.3 in the case of contamination due to water or oil. The leaves can be responsible for friction coefficient values between 0.1 and 0.2 A drastic reduction of adhesion (0.02-0.05) can occur when there is a combination of a blackish layer, due to the chemical reaction between leaves and wheel/rail steel, and light dew, rain and snow. Other studies considering different contaminants was performed in laboratory using a scaled roller-rig as shown by Bosso et al. (2014) and Bosso and Zampieri (2014). The friction coefficient is extremely variable as the weather conditions and the elements present at the contact change. Degraded adhesion is very complex to model due to the re-adhesion phenomenon, as shown by Bosso et al. (2018, 2019): in fact, when a vehicle travels along a section of contaminated track, the longitudinal forces that develop between the wheel and the rail and the high sliding values reached produce a partial removal of the contaminant layer. The result is therefore a cleaning both of the wheel, which therefore recovers adherence, and of the rail: consequently, the wheels at the rear of the vehicle do not experience such contamination thanks to the passage of the previous wheels. The phenomenon of adhesion recovery must not be confused with the re-adhesion phenomenon due to the intervention of mechatronic systems, such as WSP and antiskid systems.

The work describes a numerical model that allows to evaluate the dynamics of the vehicle during the braking operation and to correlate the pressure to the brake cylinder, which is related to the braking forces, and the angular velocities measured on the axles of the vehicle, in order to estimate adhesion coefficient. The model is developed considering the experimental measurements in braking conditions in a degraded environment for different trains with different compositions, and an automatic data analysis routine is developed to estimate the main quantities of interest. The task is the determination of the adhesion characteristic (coefficient of adhesion as a function of creepage) comparing it with the models available from studies present in the literature. The results of the work show that the adherence available on each axis of the vehicle in degraded conditions is different. The first wheelsets of the vehicle have a reduced adherence compared to the following ones. Analyzing the experimental results, the mutual influence between the different wheelsets, due to the "cleaning" effect that the first wheelsets operate on the rail, has an important influence on the vehicle braking efficiency.

Nomenclature

WSP	wheel slide protection
FM	friction modifier
TBM	third body material
μ	wheel-rail friction coefficient
F_{BK}	braking force
M	mass acting on the wheelset
p_{cyl}	pressure in the brake cylinder
μ_{pad}	disk-pad friction coefficient
F_B	clamping force
F_Z	actuator force
$\dot{U}$	caliper ratio
η	caliper efficiency
A_{BK}	effective thrust area of the actuator
F_{PRF}	return force of the cylinder spring
R	cylinder ratio

μ_C	efficiency of the cylinder
F_{SARF}	slack adjuster return spring force
F_{RNRF}	rear nut return spring force
F_{tx}	wheel-rail longitudinal friction force
n_{ks}	number of disks per wheelset
r_b	radius of application of the braking force
d_w	diameter of the wheel
$\ddot{U}_B$	brake transmission ratio
N	vehicle axle-load
ξ	longitudinal creepage
V_{train}	vehicle velocity
ω_w	wheelset angular velocity
r_w	wheel rolling radius

2. Reference vehicles and tests on track under contaminated conditions

The experimental data, provided by Faiveley, are braking test records carried out for two types of vehicle. The first vehicle is the ETR 1000, the commercial name of the Frecciarossa 1000 high-speed train, designed and produced for Trenitalia by the Ansaldo Breda-Bombardier consortium. The ETR 1000 is a high-speed train with multiple electrical units with a maximum speed of 360 km/h. The configuration of the train coaches, shown in Fig. 1, foresees the presence of 8 coaches (alternatively powered and trailed), as described by Faiveley (2015):

- DM1 e DM8: locomotives with cab and sandbox;
- TT2 e TT7: trailed coaches with hand brake device;
- M3 e M6: powered coaches;
- T4 e T5: trailed coaches with pantograph and auxiliary air compressor.

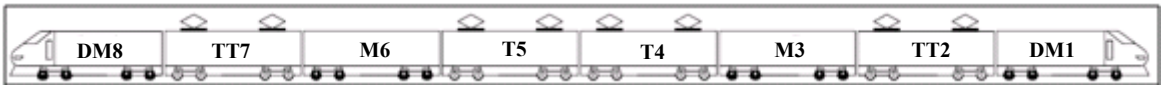

Fig. 1. Architecture and layout of the ETR 1000 train.

Tab. 3 shows the main parameters of the vehicle.

Table 3. Main parameters of the ETR 1000 vehicle.

Parameter	Value	Unit	Description
D_wheel	0.92	[m]	Wheel diameter
R_friction	0.294	[m]	Braking force radius
M	62 000	[kg]	Coach mass
J	37	[kg m2]	Wheelset moment of inertia
S	1.435	[m]	Gauge
P	9.8	[MW]	Continuous power

The experimental data, analyzed in this work, were acquired during on track tests of the train WSP system. Degraded adhesion conditions were reproduced by means of a solution of water and soap deposed on the rail by a specific system installed on the vehicle and near to the leading wheelset.

The second train whose braking records will be analyzed in this work is the Régiolis train, name of the French regional train built for SNCF by the Alstom consortium. The train, which is part of the Alstom family of Coradia Polyvalent, can travel up to a commercial speed of 160 km/h in both electric and hybrid versions, as shown by

Faiveley (2010). Fig. 2 shows a layout of the vehicle composed of 6 coaches for a total number of 16 wheelsets, identified by the letters of the alphabet from A to P. The vehicle has the possibility of movement in both directions and the numbers 1 and 2 indicate the running direction. On the other hand, analyzing the type of braking system installed, we highlight the following differences compared to the ETR 1000:

- On the driving wheelsets (axes A, B, G, H, O, P shown in black) there is the simultaneous presence of the contribution of the electropneumatic EP and ED electrodynamic brake;
- On the second (O) and second-to-last (P) wheelset the vehicle is equipped with the EP electro-pneumatic brake, ED electrodynamic brake and the DB brake;
- Two sanding systems on the A and P wheelsets.

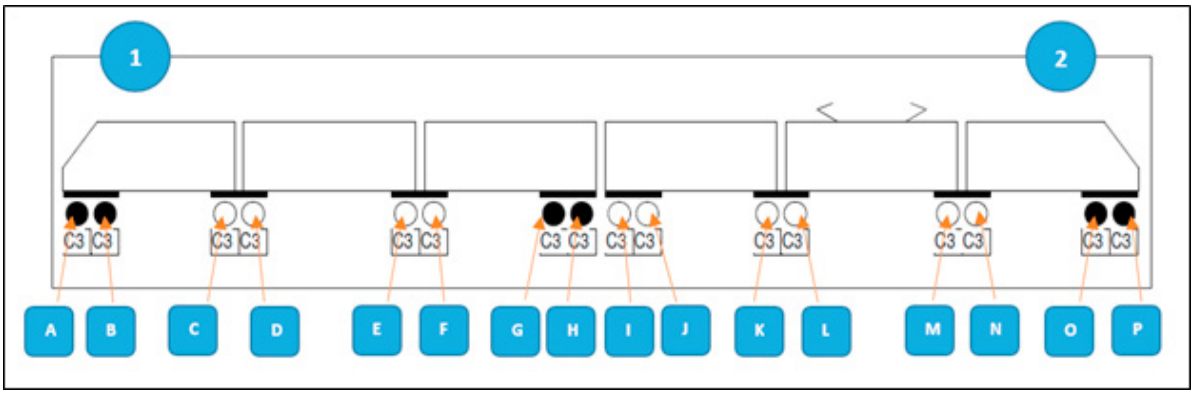

Fig. 2. Architecture and layout of the Règiolis train.

The axle-load is of 20 tons approximately. As for traction, the Régiolis has two versions: electric or dual mode (with voltage at 25 kV or 1500 V). The vehicle composition is as follows:

- 3 motor bogies;
- 1 trailed bogie;
- 4 trailed Jakobs' type bogies.

The experimental data, analyzed in this work, were acquired during on track tests of the train WSP system. Also, in this case the data is acquired by means of a control unit installed on the vehicle coach. Unlike the previous train, it is specified that in this test session the conditions of degraded adhesion are reproduced not only with soap, but also with oil. In this regard it should be noted that, like the tests on the ETR 1000, the soap is injected near the leading wheelset between the wheel and the rail. Fig. 3 shows a picture of system used to spread the soap on the rail.

As regards the adhesion tests with oil contamination, they are not carried out by injection of contaminant, but simply by dirtying a specific section of the rail on which the train will subsequently run (contaminated section of track between a minimum of 20 to a maximum of 500 m, with a minimum braking speed of 100 km/h).

Fig. 3. System used to spread the soap on the rail during the experimental tests.

3. Analysis and discussion of the experimental data

The acquired data, recorded in real time, comes from acquisitions through sensors on all 16 wheelsets. The acquired data is processed by the control unit installed on vehicle coach which provides the following results:

- Pressure in the brake cylinders for each axle p_cyl [bar];
- Angular speed of each wheelset vites_fc_ax [km/h];
- Angular acceleration of each wheelset acc_wheel [m/s^2];
- Vehicle speed calculated by the WSP vref [m/s];
- Vehicle speed measured by the GPS sensor vtrain [m/s];
- Sampling period time_camp [s];
- Safety loop safety_loop [-];
- Vehicle deceleration dec_train [m/s^2];
- Braking force provided by the electrodynamic brake ed [N].

In braking conditions, the wheel-rail adhesion coefficient μ is a function of the braking force F_{BK} and of the mass acting on the wheelset M, see Eq. 1.

$$\mu = f(F_{BK}, M) \tag{1}$$

In general, the braking force F_{BK} is modeled as a function dependent on the pressure of the brake cylinder p_{cyl} and the disc-pad friction coefficient μ_{pad}, as described by Eq. 2.

$$F_{BK} = f\ (p_{cyl}, \mu_{pad}) \tag{2}$$

The clamping force F_B applied to the pad can be obtained using Eq. 3, reported in the Faiveley (2006) dossier.

$$F_B = F_Z * \ddot{U} * \eta \tag{3}$$

In Eq. 3 the term F_z is the force generated by the actuator, while $\ddot{U}$ and η are the caliper ratio and the caliper efficiency, respectively. The force F_z of the actuator can be determined by Eq. 4, where A_{BK} is the effective thrust area of the actuator, F_{PRF} is the return force of the cylinder spring, R is the ratio of the cylinder, μ_C is the efficiency of the cylinder, F_{SARF} is the slack adjuster return spring force and F_{RNRF} is the rear nut return spring force.

$$F_z = \left[\left(A_{BK} * p_{cyl} * 10 - F_{PRF} \right) * R * \mu_C \right] - F_{SARF} - F_{RNRF} \tag{4}$$

As an alternative to Eq. 2 the clamping force can be determined in a simplified way by Eq. 5, which is only a function of the pressure of the brake cylinder p_{cyl}.

$$F_B(kN) = \frac{p_cyl(bar) - 0.1740}{0.1565} \tag{5}$$

Once the clamping force is known, it is possible to calculate the wheel-rail longitudinal tangential force acting on each wheelset by means of Eq. 6.

$$F_{tx} = F_B * \mu_{pad} * n_{KS} * \left(2 * \frac{r_B}{d_W} \right) * \ddot{U}_B \tag{6}$$

In Eq. 6 the term n_{KS} is the number of disks per wheelset, r_B is the radius of application of the braking force, d_w is the diameter of the wheel and $\ddot{U}_B$ is the eventual transmission ratio in the case in which the brake disks are not directly installed on the wheelset. Calculated the tangential friction force it is possible to evaluate the adhesion coefficient of the *i*-th axis using Eq. 7, where N_i is the normal load acting on the wheelset.

$$\mu_i = \frac{F_{tx,i}}{N_i} \tag{7}$$

In order to take into account the load transfers during braking operations, a simplified model of the vehicle has been used. The model allows to recalculate the normal load acting on each axle according to the deceleration of the vehicle. The creepage necessary to build the adhesion characteristic is calculated from the vehicle V_{train} speed, measured with the GPS sensor, and from the angular speed of the wheelset ω_W, measured by the sensor included in the WSP system, see Eq. 8.

$$\xi = \frac{V_{train} - \omega_W * r_W}{V_{train}} \tag{8}$$

The tests on track have been carried out to evaluate the WSP system, which acting directly on the brake cylinder pressure affects the adhesion characteristic. To overcome this problem, specific working points, called critical points, are identified. These points are characterized by having a variation in the creepage concavity (the creepage first derivative changes sign from positive to negative or vice versa). Considering these working points, the adhesion coefficient reaches a maximum value equal to the wheel-rail friction coefficient because the used adhesion reaches a value equal to the available one. From one critical point to the next, therefore, there is the intervention of the WSP, which influences the adhesion conditions. To study, therefore, the adhesion curve, the critical points, which are not affected by the WSP system, are selected. In Fig. 4 the speed of the first wheelset of the vehicle (blue line) is shown as an example with the indication in green of the critical points. The curve refers

to a test carried out on the ETR 1000 vehicle in the case of contamination with a mixture of water and soap. The curve in black color represents the speed of the vehicle.

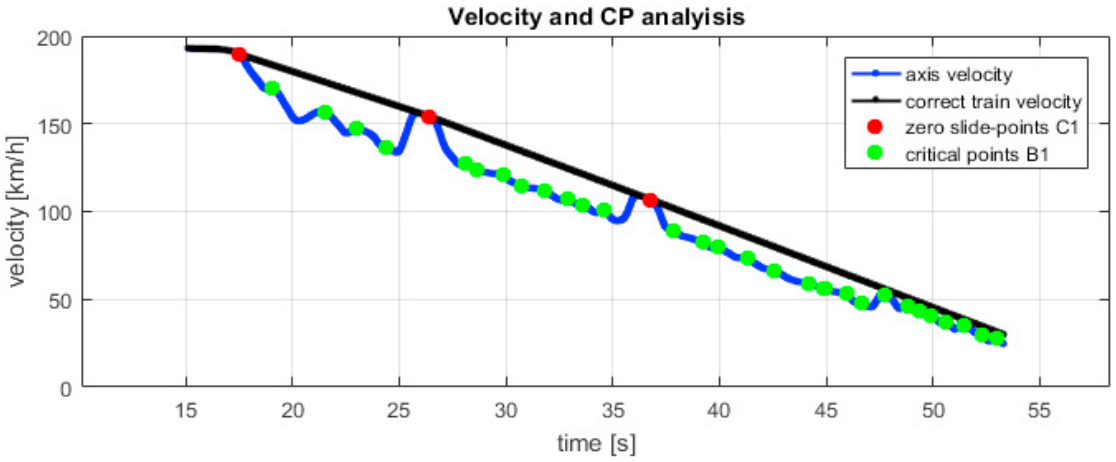

Fig. 4. Speed of the leading wheelset (blue line) and of the vehicle (black line). The critical points are indicated with green markers.

The critical points in red color represent the points which are characterized by low values of sliding speed (between 0 km/h and 0.2 km/h). They correspond to points where there is predominantly a condition of adhesion within the contact area and they are used to build the adhesion characteristic for low creepage values.

On each critical point the adhesion coefficient is calculated according to Eq. 7, while the longitudinal creepage is calculated through Eq. 8. The critical points are then fitted to obtain the adhesion characteristic. The interpolation of the experimental points is performed using the expression of the tangential force defined by Polach (2010), see Eq. 9. Alternatively, the contact model developed by the authors and described in Bosso et al. (2002, 2012) and Bosso and Zampieri (2018) can be used to fit the experimental results.

$$\mu = \mu_0 * \frac{1 - e^{-\left(\frac{|K*\xi|}{\mu_0} * \left(1 + K_{rozv} * |DV|\right)\right)}}{1 + K_{rozv} * |DV|} \tag{9}$$

In Eq. 9 μ_0 is the static friction coefficient, K is the Kalker coefficient, K_{rozv} is a parameter that considers the dependency of the friction coefficient from the sliding speed and DV is the sliding speed. The experimental points are interpolated by varying the coefficients K, μ_0 and K_{rozv}.

Fig. (5) shows the adhesion curves of the first four wheelsets of the ETR 1000 train obtained during a braking test starting from a speed of 150 km/h in case of soap and water contamination.

The red curves shown in Fig. 5 represent the adhesion characteristics obtained by interpolating the experimental data. The values of the curve coefficients are shown in Tab. 4.

Table 4. Coefficients of the Polach's law for the 4 wheelsets.

BS 150 km/h	μ0	K	Krozv
AX 1	0.1497	30.00	0.0291
AX 2	0.1497	30.00	0.0325
AX 3	0.1542	29.99	0.0308
AX 4	0.1593	29.99	0.0286

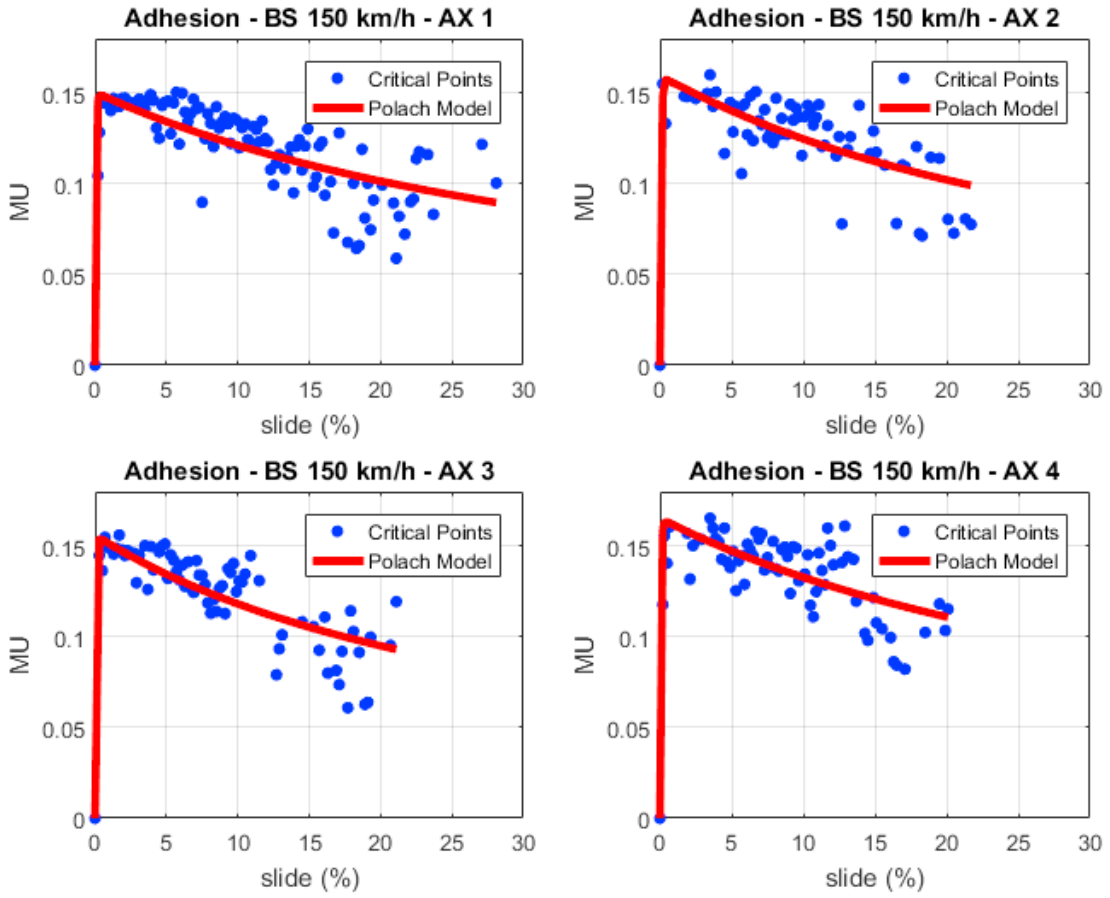

Fig. 5. Adhesion curves of the first four wheelsets of the ETR 1000 vehicle obtained during a braking test starting from a speed of 150 km/h in case of soap and water contamination.

Observing the values of the static friction coefficient μ_0 it is evident that the higher values are measured in correspondence of the wheelsets 3 and 4 which run on the contaminated track section after wheelsets 1 and 2. This increase of the adhesion coefficient is due to the cleaning effect that the first wheelsets of the vehicle perform during the passage on the contaminated rails (adhesion recovery phenomenon). The adhesion recovery is even more evident if we consider Fig. 6, where the adhesion characteristics are shown on the same diagram.

Considering the Règiolis vehicle and analyzing the case of contamination of the rail with soap and water, it is still possible to observe the phenomenon of adhesion recovery as shown in Fig. 7. In this case the axes M and N which encounter the contaminated rail subsequently to the axes P and O appear to have a better adhesion. The adhesion recovery is more evident for the Règiolis train rather than the ETR probably due to the different tested speed values. Furthermore the two tests were carried out in two separate test campaign, hence the friction condition could slightly differ. For the Règiolis vehicle, tests are also available with oil as a contaminant. The results for this type of contaminant are shown in Fig. 8. In this case the phenomenon of adhesion recovery is not present and the adhesion among the four wheelsets has a random distribution. In fact this type of contaminant is difficult to remove from the rail so that the following wheelsets do not exploit the cleaning effect.

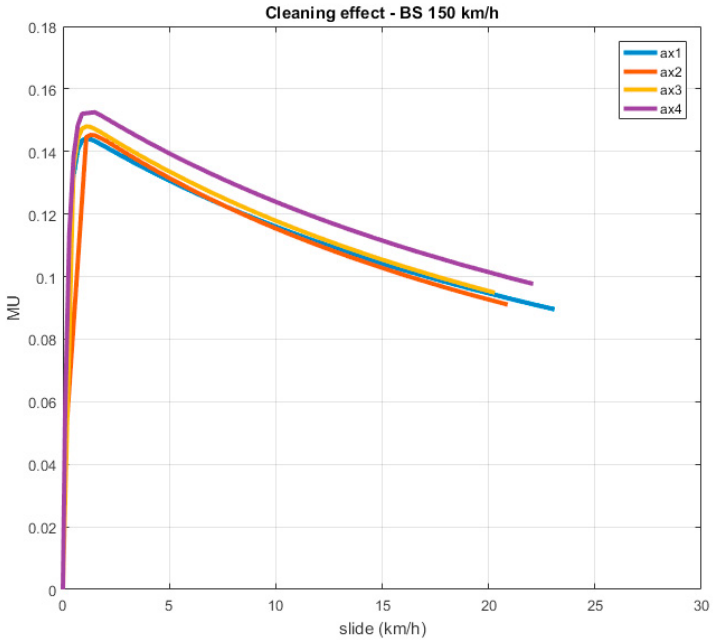

Fig. 6. Comparison of the adhesion curves of the first four wheelsets of the ETR 1000 vehicle obtained during a braking test starting from a speed of 150 km/h in case of soap and water contamination.

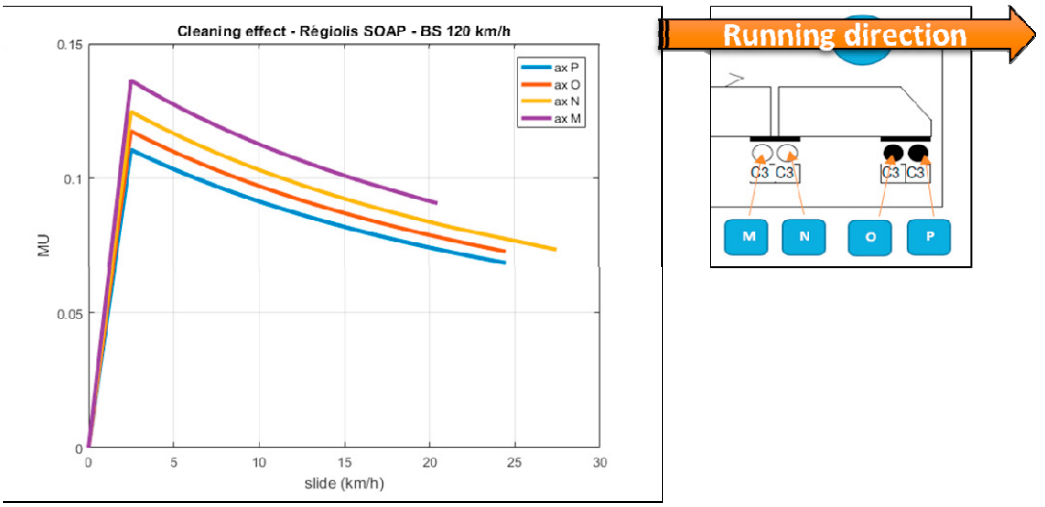

Fig. 7. Comparison of the adhesion curves of the first four wheelsets of the Règiolis vehicle obtained during a braking test starting from a speed of 120 km/h in case of soap and water contamination.

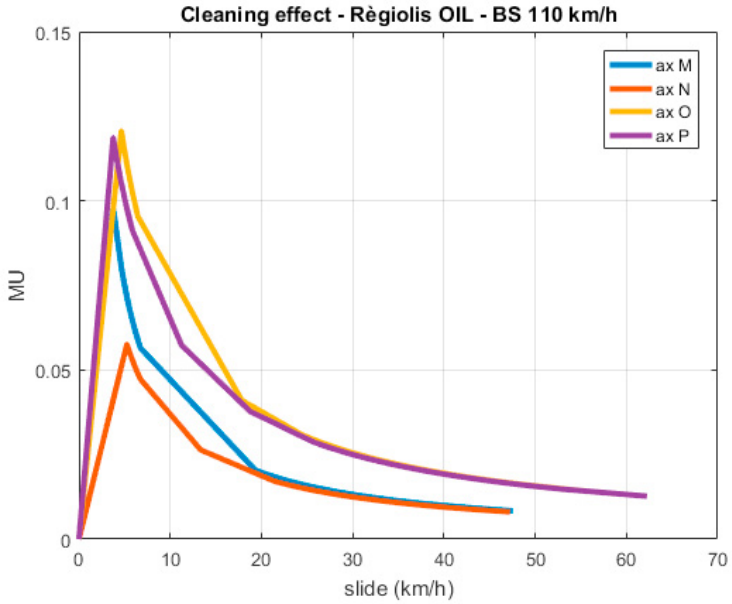

Fig. 8. Comparison of the adhesion curves of the first four wheelsets of the Règiolis vehicle obtained during a braking test starting from a speed of 120 km/h in case of oil contamination.

4. Conclusions

The paper proposes an experimental approach to study railway adhesion under degraded conditions during the braking maneuver. The work uses the experimental data recorded during tests to calibrate and verify the WSP system of two different types of vehicles: the ETR 1000 high-speed train and the Règiolis regional train. Regarding the dependence of adhesion on the type of contaminant, the analysis for the ETR 1000 vehicle during a test with water and soap contamination, highlighted a peak of the adhesion coefficient on variable values, based on the axis considered, between 0.16 and 0.14. The work also shows the adhesion values coming from braking records on the regional Règiolis train carried out both on oil and soap. Tests carried out on oil contaminants have shown a lowering of the adhesion values, especially for high creepage levels. Furthermore, the maximum of adhesion for water and soap tests are very close to the values measured on the ETR 1000 high-speed vehicle considering the same type of contaminant. Experimental measurements demonstrate that the adhesion recovery occurring on the last wheelsets of the vehicle (thanks to the passage of the previous wheels) is significant and being able to quantify this phenomenon would allow to optimize the WSP algorithms, with a consequent improvement in vehicle performance during the braking maneuver. The results also show that the adhesion recovery phenomenon is well quantifiable in the case of soap-based contaminants, while the phenomenon was not observed in the case of contamination with oil. This type of contaminant is in fact particularly difficult to remove from the rail.

Acknowledgements

The activity was developed in a close collaboration between the R&D department, brake & safety division, of Faiveley Transport (now Wabtec Corporation) of Piossasco (TO), and the railway research group of the Politecnico di Torino. The authors thank Eng. Matteo Frea and Eng. Luc Imbert from Wabtec for the experimental data provided and for their support in data analysis.

References

Bosso N., Zampieri N., 2018. A Novel Analytical Method to Calculate Wheel-Rail Tangential Forces and Validation on a Scaled Roller-Rig, Advances in Tribology, vol. 2018, art. no. 7298236, 1-11.

Bosso, N., Gugliotta, A., Magelli, M., Zampieri N., 2019. Experimental Setup of an Innovative Multi-Axle Roller Rig for the Investigation of the Adhesion Recovery Phenomenon, Experimental Techniques.

Bosso, N., Magelli M., Zampieri N., 2019. Investigation of adhesion recovery phenomenon using a scaled roller-rig, Vehicle System Dynamics.

Bosso, N., Gugliotta, A., Somà, A., 2002. Introduction of a wheel-rail and wheel-roller contact model for independent wheels in a multibody code, ASME/IEEE 2002 Joint Rail Conference, RTD 2002, 151-159.

Bosso, N., Gugliotta, A., Zampieri, N., 2012. RTCONTACT: An efficient wheel-rail contact algorithm for real-time dynamic simulations, Joint Rail Conference, JRC 2012, 195-204.

Bosso, N., Gugliotta, A., Zampieri, N., 2014. Study of adhesion and evaluation of the friction forces using a scaled roller-rig, 5th World Tribology Congress, WTC 2013, 3, 2640-2643.

Bosso, N., Gugliotta, A., Zampieri, N., 2015. Strategies to simulate wheel-rail adhesion in degraded conditions using a roller-rig, Vehicle System Dynamics, 53(5), 619-634.

Bosso, N., Gugliotta, A., Zampieri, N., 2016. A test rig for multi-wheelset adhesion experiments, Civil-Comp Proceedings, 110.

Bosso, N., Gugliotta, A., Zampieri, N., 2018. Study of the wheel-rail adhesion under degraded conditions using a multi-axles roller-rig, The Dynamics of Vehicles on Roads and Tracks, 2, 803-808.

Bosso, N., Zampieri, N., 2014. Experimental and numerical simulation of wheel-rail adhesion and wear using a scaled roller rig and a real-time contact code, Shock and Vibration, 2014, art. no. 385018, 1-14.

Faiveley Transport, 2006. Sistemi di controllo del freno ferroviario, Centenario Faiveley Transport.

Faiveley Transport, 2010. Brake Calculation Régiolis, project number FR02404.

Faiveley Transport, 2015. Brake Calculation ETR1000 V300 Zefiro, project number IT10002.

Fulford, C. R., 2004. Review of low adhesion research, Report published by the Railways Safety and Standards Board.

Harmon, M., Lewis, R., 2016. Review of top of rail friction modifier tribology, Tribology - Materials, Surfaces and Interfaces, 10(3), 150-162.

Lewis, R., Olofsson, U., 2009. Basic tribology of the wheel-rail contact, Wheel-Rail Interface Handbook, 34-57.

Moore, D. F., 1975. Chapter 14 - Transportation and Locomotion, Principles and Applications of Tribology, 302-330.

Olofsson U., Zhu Y., Abbasi S. et al., 2013. Tribology of the wheel-rail contact-aspects of wear, particle emission and adhesion, Vehicle System Dynamics, 51(7), 1091-1120.

Olofsson, U., 2009. Adhesion and friction modification, Wheel-Rail Interface Handbook, 510-527.

Polach, O., 2010. Characteristic parameters of nonlinear wheel/rail contact geometry, Vehicle System Dynamics, 48(supp 1), 19-36.

UIC, 2016. Brakes Manufacturing specifications for various brake parts – Wheel Slide Protection device (WSP), 3rd edition.

UNI, 2011. Norma specifica per i criteri minimi per l'accettazione del sistema frenante e l'approvazione di un sistema di antipattinamento nuovo, EN 15595.